ACS Chemical Neuroscience

Research Article

pubs.acs.org/chemneuro

Light-Triggered Modulation of Cellular Electrical Activity by Ruthenium Diimine Nanoswitches

Joyce G. Rohan,[†,⊥,○] Y. Rose Citron,[†,○] Alec C. Durrell,[‡] Lionel E. Cheruzel,[#] Harry B. Gray,[‡] Robert H. Grubbs,[§] Mark Humayun,[∥] Kathrin L. Engisch,[⊥] Victor Pikov,[▽] and Robert H. Chow*[,†]

[†]Department of Physiology and Biophysics, Zilkha Neurogenetic Institute, Keck School of Medicine, University of Southern California, Los Angeles, California 90089-2821, United States

[‡]Beckman Institute and [§]Arnold and Mabel Beckman Laboratory of Chemical Synthesis, Division of Chemistry and Chemical Engineering, California Institute of Technology, Pasadena, California 91125, United States

[∥]Doheny Eye Institute, Keck School of Medicine, University of Southern California, Los Angeles, California 90033, United States

[⊥]Wright State University, Dayton, Ohio 45435, United States

[#]Department of Chemistry, San José State University, San José, California 95192-0101, United States

[▽]Huntington Medical Research Institute, Pasadena, California 91105, United States

ABSTRACT: Ruthenium diimine complexes have previously been used to facilitate light-activated electron transfer in the study of redox metalloproteins. Excitation at 488 nm leads to a photoexcited state, in which the complex can either accept or donate an electron, respectively, in the presence of a soluble sacrificial reductant or oxidant. Here, we describe a novel application of these complexes in mediating light-induced changes in cellular electrical activity. We demonstrate that RubpyC17 ($[Ru(bpy)_2(bpy\text{-}C17)]^{2+}$, where bpy is 2,2′-bipyridine and bpy-C17 is 2,2′-4-heptadecyl-4′-methyl-bipyridine), readily incorporates into the plasma membrane of cells, as evidenced by membrane-confined luminescence. Excitable cells incubated in RubpyC17 and then illuminated at 488 nm in the presence of the reductant ascorbate undergo membrane depolarization leading to firing of action potentials. In contrast, the same experiment performed with the oxidant ferricyanide, instead of ascorbate, leads to hyperpolarization. These experiments suggest that illumination of membrane-associated RubpyC17 in the presence of ascorbate alters the cell membrane potential by increasing the negative charge on the outer face of the cell membrane capacitor, effectively depolarizing the cell membrane. We rule out two alternative explanations for light-induced membrane potential changes, using patch clamp experiments: (1) light-induced direct interaction of RubpyC17 with ion channels and (2) light-induced membrane perforation. We show that incorporation of RubpyC17 into the plasma membrane of neuroendocrine cells enables light-induced secretion as monitored by amperometry. While the present work is focused on ruthenium diimine complexes, the findings point more generally to broader application of other transition metal complexes to mediate light-induced biological changes.

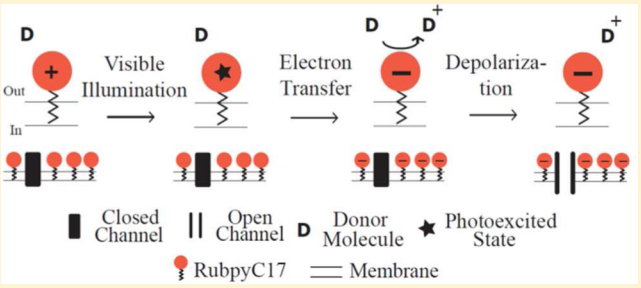

KEYWORDS: *Optogenetics, metal-diimine, action potentials, neuroendocrine cells, secretion, light*

Development and application of optical approaches to control cellular activity, particularly neuronal activity, is a rapidly growing field. Several groups have pioneered approaches to control cellular membrane potential by heterologously expressing light-responsive proteins in cells to render them light-sensitive.[1−15] For example, investigators have cloned naturally light-sensitive transporters found in non-mammalian species, such as channelrhodopsins and halorhodopsins, for heterologous expression in mammalian cells.[6−11,13−15] Another light-sensitive class of proteins that has also been cloned and expressed heterologously is melanopsin, a photoisomerizable pigment that signals through the G protein of the G_q family in a specialized subset of retinal ganglion cells.[12]

Other groups have employed synthetic chemistry approaches that avoid expression of foreign proteins. For example, some groups have synthesized photolabile "caged" neurotransmitters that liberate the neurotransmitter upon photolysis by UV illumination,[16,17] thereby enabling light to activate ligand-gated ion channels. Another synthetic chemistry approach involves use of small diffusible "photoswitch" compounds that act directly on native ion channels to induce light-triggered changes in membrane potential. One particularly promising class of photoswitches is based on photoisomerization of azobenzene. When covalently attached to one or two potassium channel

Received: November 27, 2012
Accepted: January 18, 2013
Published: February 18, 2013

blocker moieties (tetraethylammonium), these azobenzene compounds are internalized by cells and interact with potassium channels to either block or unblock outward potassium flux, when alternating illumination wavelengths between 500 and 380 nm.[18] Azobenzene compounds have also been covalently attached to ion channels at cysteine residues, introduced by site-directed mutagenesis, to enable activation or block of either voltage-gated or ligand-gated ion channels.[2,3]

Though successful in modulating cellular electrical activity and offering useful tools for basic research, all the approaches described above require either heterologous expression of high levels of foreign proteins or excitation by ultraviolet illumination and, therefore, would not be easily translated to clinical applications.

Recently, an approach was described involving a new class of synthetic photoswitches that generate charge separation upon illumination at visible wavelengths. Ferrocene-porphyrin-C60 compounds targeted to cell membranes using cell-penetrating, high-density lipoprotein induce a light-dependent membrane depolarization, though the mechanism was not thoroughly examined.[19] A limitation of the ferrocene-porphyrin-C60 compounds at the moment is that their action is confined to inhibiting potassium channels, and hence they can only depolarize the cell.

Here, we report on another class of synthetic photoactivatable nanoswitches that alter cell membrane potentials. Ruthenium-diimine complexes, which have previously been used to facilitate light-activated electron transfer in redox metalloproteins, can be excited in the blue region of the visible spectrum.[20−31] The complex employed here is $[Ru(bpy)_2(bpy\text{-}C17)]^{2+}$,where bpy is 2,2′-bipyridine and bpy-C17 is 4-heptadecyl-4′-methyl-2,2′-bipyridine, which will be referred to as RubpyC17. Illumination generates a photoexcited complex that can either accept or donate an electron, depending on whether a sacrificial reductant (e.g., ascorbate) or oxidant (e.g., ferricyanide) is present.[32] The addition of a 17-carbon aliphatic chain (C17) to one of the three bipyridine (bpy) ligands in RubpyC17 serves to anchor the complex in the cellular plasma membrane. Light-activated electron transfer to or from this membrane-anchored complex alters the charge of the cell membrane capacitor, inducing either a depolarization in the presence of excess reductant or hyperpolarization in the presence of excess oxidant. We further show that this light-induced change in membrane potential is sufficient to open and close voltage-gated ion channels such that we can regulate and manipulate action potential firing rate and secretion in neuroendocrine cells.

RESULTS AND DISCUSSION

Membrane Integration of RubpyC17. The excitation and emission spectra, as well as the structure of RubpyC17 are shown in Figure 1A. RubpyC17 applied to the bath at a final concentration of 10 μM rapidly and stably incorporates into mammalian cell membranes as shown by plasma membrane-localized luminescence[30,31] (Figure 1B). Illustrated here are rat insulinoma (INS) cells (Figure 1B, top), human embryonic kidney (HEK293T) cells (Figure 1B, middle), and primary cultured mouse chromaffin cells (Figure 1B, bottom). None of these cell types exhibited significant autofluorescence or autoluminescence in the red channel, as shown by lack of emission collected from cells not exposed to RubpyC17. All cell types preserved morphology for at least 10 min. Incorporation into the plasma membrane was stable as membrane luminescence was still observed at 10 min after RubpyC17 removal from the bath solution. The predicted light-induced electron transfer is depicted in Figure 1C.

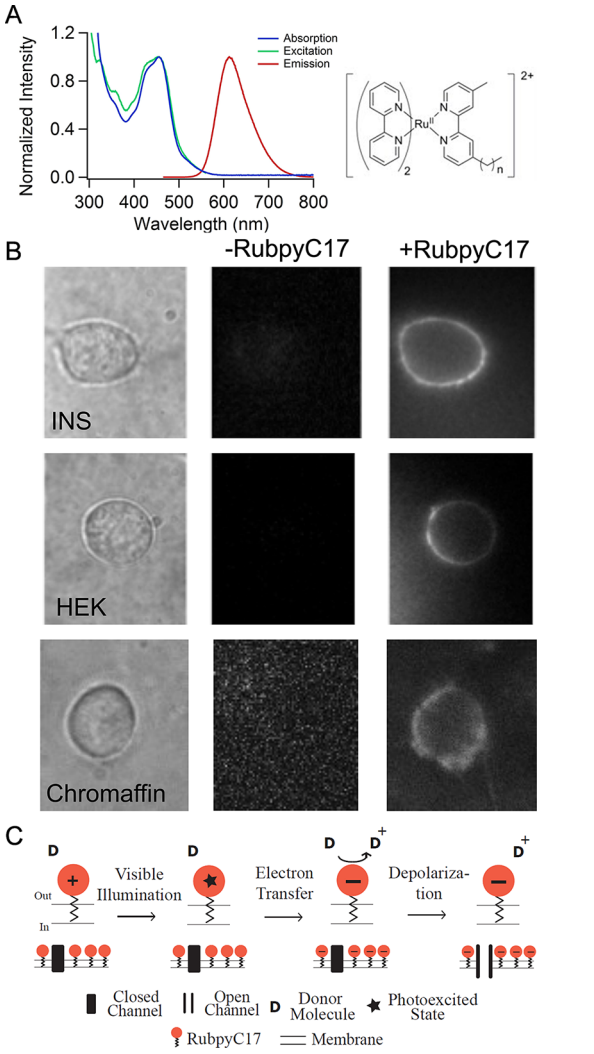

Figure 1. Incorporation of RubpyC17 in plasma membranes of live cells. (A) Normalized absorption (blue), excitation (green), and uncorrected emission (red) spectra of RubpyC17 and structure of RubpyC17, where n = 16. (B) Images obtained of INS (top row), HEK293T (middle row), and chromaffin (bottom row) cells under brightfield illumination (left column), before addition of RubpyC17 (middle column) and immediately after addition of 10 μM RubpyC17 (right column). Luminescent images (right column) were obtained by collecting emitted light using a red filter set following excitation with 488 nm light from an argon ion laser. (C) Diagram depicting the predicted light-induced electron flow. Light illumination electronically excites RubpyC17 to a charge transfer state that is either an electron donor or an electron acceptor. If an electron donor (reductant, represented as D in figure) is present, RubpyC17 will accept transfer of electrons from donor, creating a negative surface potential at the cell membrane, which is observed by the cell as a depolarization. This depolarization is sufficient to induce opening of voltage-gated ion channels.

Light-Triggered Changes in Membrane Potential. We next investigated whether cells treated with RubpyC17 exhibit light-induced membrane potential changes. We first tried INS and HEK cells, both cells that are not excitable under normal conditions (INS cells were maintained in low glucose, <3 mM,

dx.doi.org/10.1021/cn300213f | ACS Chem. Neurosci. 2013, 4, 585−593

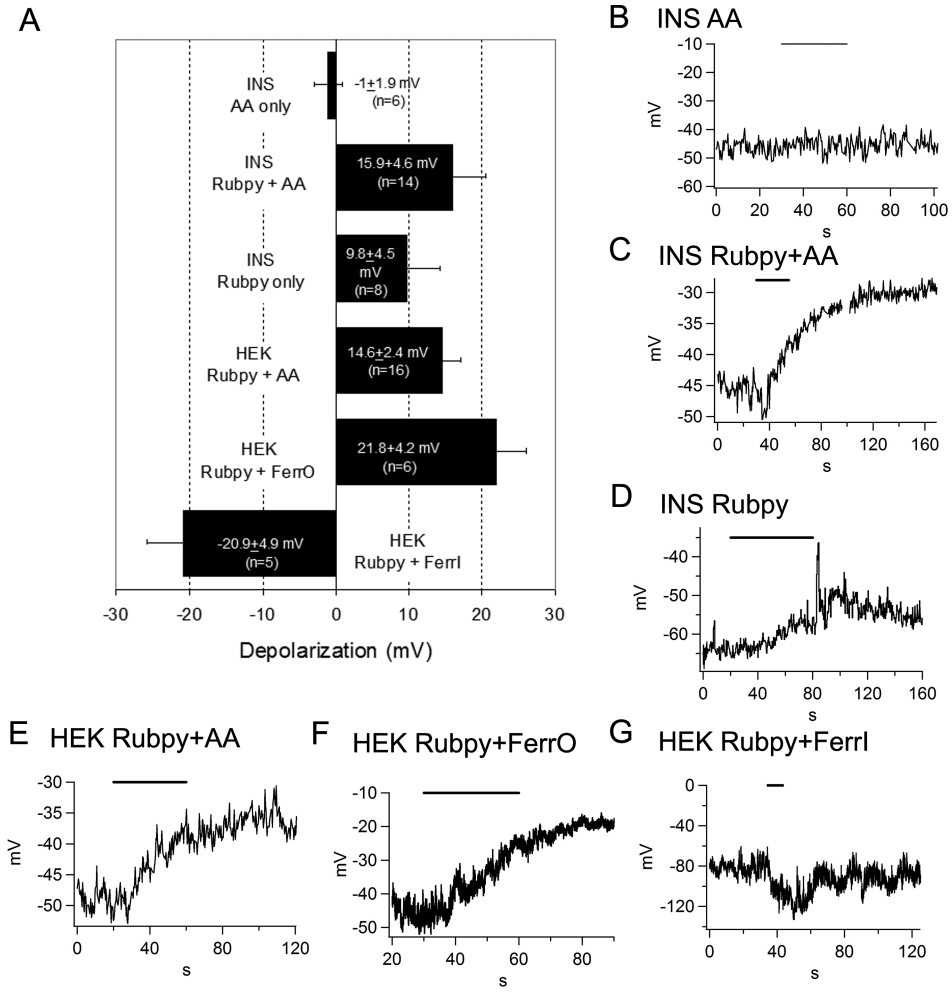

Figure 2. Bidirectional control of membrane voltage by light in cells preincubated with RubpyC17. (A) Summary bar graph showing averaged depolarization and hyperpolarization values of RubpyC17-loaded INS and HEK293T cells when stimulated by blue light illumination. (B–G) Representative traces from cells depicted in (A). (B) Membrane potential recording from an INS cell that was not exposed to RubpyC17 in the presence of 2 mM ascorbate (AA) showed no changes during light stimulation (bar). (C) Membrane potential recording from an INS cell that was transiently exposed to RubpyC17 for 2 min in the presence of 2 mM ascorbate (AA) depolarized during light stimulation (bar). (D) Membrane potential recording from an INS cell that was transiently exposed to RubpyC17 for 2 min in standard extracellular solution without supplementation of reductants or oxidants still showed light-induced depolarization. (E) Membrane potential recording from an HEK293T cell that was transiently exposed to RubpyC17 for 2 min in the presence of 2 mM ascorbate (AA) depolarized during light stimulation (bar). (F) Membrane potential recording from an HEK293T cell that was transiently exposed to RubpyC17 for 2 min in the presence of an alternate reductant, 0.1 mM ferrocyanide (ferrO) depolarized during light stimulation (bar). (G) Membrane potential recording from an HEK293T cell that was transiently exposed to RubpyC17 for 2 min in the presence of an oxidant, 0.1 mM ferricyanide (ferrI) hyperpolarized during light stimulation (bar).

to prevent action potentials). The cells were incubated in 10 μM of RubpyC17 for approximately 2 min then washed with standard extracellular solution, supplemented with 2 mM ascorbate. To monitor the plasma membrane potential, the cells were patch-clamped in whole-cell configuration in current-clamp mode and membrane voltages were recorded while illuminating the cell at 488 nm (0.46–0.48 mE s^{-1} m^{-2}).

Upon illumination, the membrane potential of INS cells increased by an average of 15.9 ± 4.6 mV in the presence of ascorbate (Figure 2A,C). In the absence of ascorbate, INS cells incubated with RubpyC17 still showed a modest increase in membrane potential upon illumination (average of 9.8 ± 4.5 mV) (Figure 2A, D). Similarly, HEK293 cells also showed light-induced depolarization of 14.6 ± 2.4 mV in the presence of ascorbate (Figure 2A,E). Control INS cells not exposed to the RubpyC17 compound showed no change in membrane potential upon illumination, with or without ascorbate (Figure 2A,B). The light-induced depolarization was also observed using ferrocyanide as reductant (Figure 2A,F).

To further test whether the change in the membrane potential was caused by electron transfer between the sacrificial redox molecules and light-activated RubpyC17, we replaced the reductant molecules in the extracellular solution with oxidant molecules, which should lead to hyperpolarization instead of depolarization upon illumination. Indeed, in the presence of 100 μM ferricyanide in the extracellular solution, illumination of cells pretreated with RubpyC17 induced a hyperpolarization of 20.9 ± 4.9 mV (Figure 2A,G).

We find that all luminescent cells undergo depolarization when illuminated for 25 s or longer when reductants (i.e., ascorbate) are present or for 10 s or longer when oxidants (i.e., ferricyanide) are present (Figure 2A). Although our data are not sufficient to address whether we can control light-induced depolarization or hyperpolarization amplitude or rate by

dx.doi.org/10.1021/cn300213f | ACS Chem. Neurosci. 2013, 4, 585–593

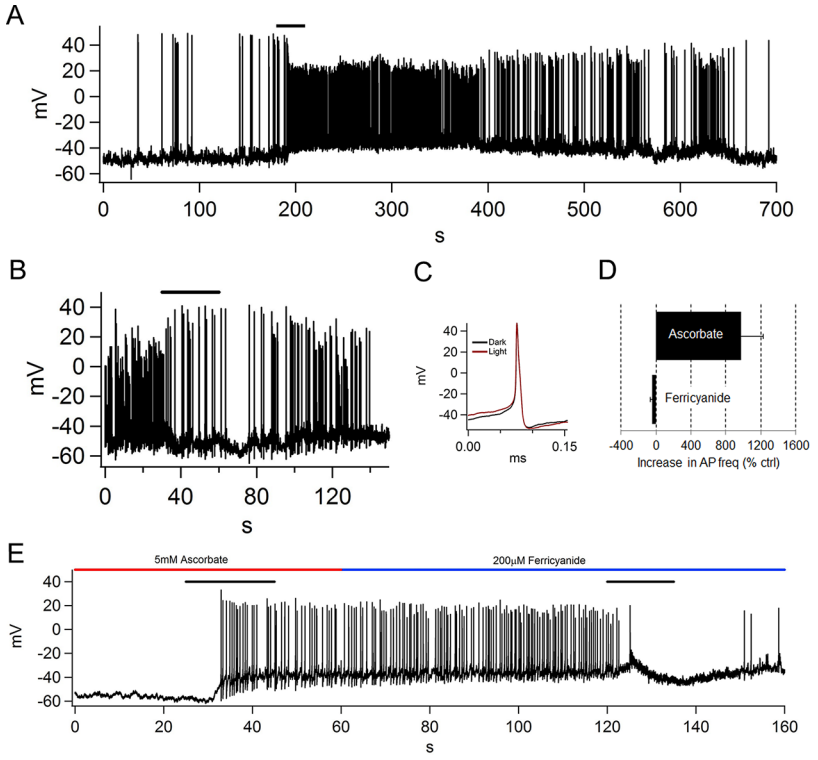

Figure 3. Bidirectional control of action potential firing rate in mouse chromaffin cells preincubated with RubpyC17. (A) In the presence of 5 mM ascorbate, blue light illumination increased the rate of action potential firing by chromaffin cells incubated in 900 nM RubpyC17 for 30 min. (B) In the presence of 0.1 mM ferricyanide, blue light illumination decreased the rate of action potential firing by chromaffin cells incubated in 450 nM RubpyC17 for 30 min. (C) There were no obvious changes in action potential waveforms of RubpyC17-treated cells before and during light illumination. (D) Bar graph measuring the percent increase relative to control (dark) of action potential firing rate during light illumination, in chromaffin cells treated with RubpyC17 in the presence of 5 mM ascorbate (n = 12) and 0.1 mM ferricyanide (n = 8). (E) Blue light illumination increased the rate of action potential firing by a RubpyC17-loaded chromaffin cell (2 μM, 1.5 min) during perfusion of 5 mM ascorbate but decreased the rate of action potential firing by during perfusion of 0.2 mM ferricyanide. Bar in each trace indicates the duration of blue light illumination.

varying illumination time or intensity, they demonstrate that RubpyC17 is capable of consistently conferring light-sensitivity to cells that normally do not respond to light.

Light-Triggered Action Potentials. We next investigated the behavior of excitable cells (cells capable of firing action potentials) treated with RubpyC17. We performed perforated patch clamp recording on mouse adrenal chromaffin cells pretreated with 450−900 nM RubpyC17 for 15−30 min before beginning electrophysiological recordings. In the presence of the reductant ascorbate (5 mM), light illumination triggered action potentials or increased the rate of action potential firing most consistently with cells pretreated with 900 nM RubpyC17 (Figure 3A,D). We observed a slow, gradual reversal, on the order of seconds after light illumination was terminated (Figure 3A). There was no change in the shape of action potential waveforms due to light illumination (Figure 3C).

In the presence of the oxidant ferricyanide (100 μM), light illumination decreased the rate of action potential firing (Figure 3B,D) in mouse chromaffin cells. This finding is consistent with the observation that illumination of RubpyC17-treated INS cells in the presence of ferricyanide resulted in hyperpolarization. The dampening effect on action potential firing in chromaffin cells is slowly reversed upon termination of light illumination (Figure 3B). Increasing the ferricyanide concentration from 100 to 200 μM further suppressed action potential firing, but also caused adverse effects on cell health such that we were not able to consistently maintain a stable seal in all cells tested (not shown).

This effect on action potential firing was also observed when the cells were transiently exposed to higher concentration of RubpyC17 (2 μM) for 1.5 min prior to recording (Figure 3E). Action potential firing rate at a single chromaffin cell that was transiently exposed to 2 μM RubpyC17 undergoes light-induced increase and then light-induced decrease, when the extracellular solution initially containing the reductant ascorbate is changed for one containing the oxidant ferricyanide (Figure 3E).

Light-Triggered Secretion. Action potential firing triggers secretion of norepinephrine and epinephrine from adrenal chromaffin cells, which can be readily detected by the technique of carbon-fiber amperometry.[33,34] Mouse chromaffin cells pretreated with 2 μM RubpyC17 and illuminated at 488 nm exhibited numerous amperometric current spikes, indicative of vesicular secretion (Figure 4A,D). Control chromaffin cells not treated with RubpyC17 did not secrete in response to light (Figure 4B,D). Out of 18 RubpyC17-loaded cells tested, 15 cells (83%) experienced increased secretion by at least 100-fold during light illumination. Unlike the changes in light-induced depolarization, light-induced changes in secretion appeared to be more transient. One likely explanation is that, at any moment in time, there is only a small number of release-competent vesicles, the so-called readily releaseable pool of vesicles, and maintained stimulation causes rapid depletion of

dx.doi.org/10.1021/cn300213f | ACS Chem. Neurosci. 2013, 4, 585−593

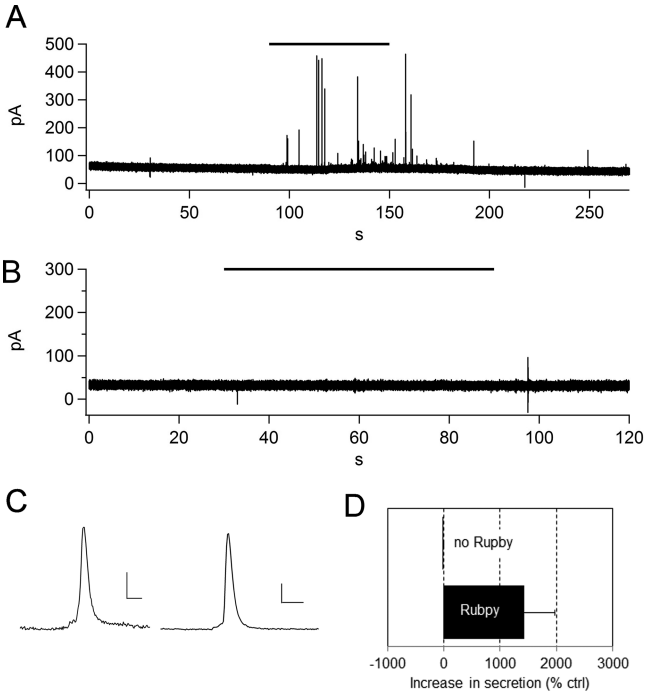

Figure 4. Light-triggered secretion in mouse chromaffin cells preincubated with RubpyC17. (A) Mouse chromaffin cells were preincubated with 2 μM RubpyC17 for 1.5 min in a modifed extracellular solution containing 20 mM KCl, and catecholamine secretion was monitored and detected using carbon fiber amperometry before, during (bar) and after blue light illumination. (B) Secretion pattern of a control mouse chromaffin cell that was not exposed to RubpyC17. (C) Examples of individual amperometric spikes elicited by light illumination in chromaffin cells treated with 2 μM RubpyC17 . Scale bars = 5 ms, 0.1 nA. (D) Bar graph measuring the percent increase relative to control (dark) of secretion spikes during light illumination in control chromaffin cells (not treated with RubpyC17) (n = 8) and RubpyC17-treated chromaffin cells (n = 18).

the readily releaseable pool of vesicles in the initial phase of stimulation.

Mechanism of Action. Our data thus far suggest that the light-induced membrane potential changes are due to electron transfer from a sacrificial redox molecule and the membrane-anchored RubpyC17 resulting in a change in the charge capacitatively stored on the cell membrane. The following two alternative explanations have been evaluated: (1) light-induced direct interaction between RubpyC17 and ion channels and (2) light-induced pore formation in the plasma membrane.

To examine whether light-activated RubpyC17 can directly interact and open or block endogeneous ion channels, we briefly preincubated HEK293T cells with RubpyC17, and patch-clamped the cells in voltage-clamp configuration. Voltage-clamp configuration allowed us to clamp the cell at a membrane potential at which most voltage-gated ion channels are closed (−80 mV). Cells treated with RubpyC17 did not exhibit light-induced changes in membrane current (Figure 5A,B). We also measured the current−voltage relationship (Figure 5C,D) as well as the steady-state voltage-dependent activation curves of RubpyC17-treated chromaffin cells in voltage-clamp mode before and during light illumination (Figure 5E). Our data suggest that the integration of RubpyC17 in the plasma membranes does not alter the biophysical properties of endogeneous ion channels.

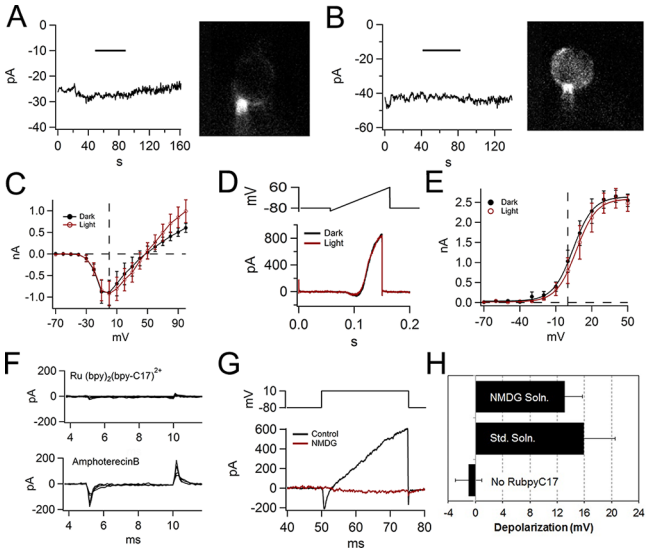

Figure 5. (A,B) Membrane current monitored in voltage-clamp mode showed that light illumination did not trigger current changes in RubpyC17-loaded INS cells. Inset images shown to the right of trace confirmed proper integration of RubpyC17 in patched cells. (C−E) The light-induced action potential firing in chromaffin cells was not due to biophysical changes in voltage-gated ion channels as there were no significant changes in current−voltage relationships (C,D) or in the steady-state activation curve (E) in RubpyC17-loaded chromaffin cells before (red, open circle) or during (red, open circle) light illumination. (C) Current−voltage relationship was obtained in voltage-clamp mode using a resting potential of −80 mV and depolarizing the cell in 10 mV increments, from −70 to 100 mV, before and during light-illumination. Peak inward currents from each stimulation jump were plotted against corresponding stimulating voltages (n = 6). (D) Current−voltage relationship was obtained in voltage-clamp mode using a resting potential of −80 mV and stimulating the cell with a ramping depolarization ranging from −100 mV to +60 mV, before and during light illumination. Data from representative cell are shown (n = 5). (E) Steady-state activation curve was generated by measuring the peak tail current immediately following a short 0.5 ms depolarizing jumps to −70 to +100 mV from a resting potential of −80 mV (n = 5). (F) Inclusion of 18 μM of RubpyC17 (top trace) in the intracellular solution inside the patch pipet did not perforate chromaffin cells (n = 10), unlike inclusion of amphoterecin B (bottom trace, n = 4). Currents resulting from capacitor-like behavior of chromaffin cell membranes during hyperpolarizing jumps to −85 mV from a resting membrane potential of −80 mV were recorded 5 min following giga-seal formation for amphoterecin B (bottom trace) or 10 min following giga-seal formation for RubpyC17 (top trace). (G) Substitution of sodium ions by NMDG and potassium by cesium dramatically reduced both inward and outward current in INS cells. (H) In external solution where NMDG was substituted for sodium ions, and cesium for potassium ions, RubpyC17-loaded INS cells still underwent light-induced depolarization in the presence of ascorbate (NMDG solution: n = 5, standard solution: n = 14, control cells not exposed to RubpyC17: n = 6).

Finally, to test whether illumination of RubpyC17 incorporated in cell membranes causes nonspecific membrane poration or other damage, we applied 18 μM RubpyC17 inside a patch pipet and attached this pipet by gigaseal to a cell in the cell-attached configuration (the same configuration used routinely for perforated-patch recording).[35] We illuminated the cell with blue light then applied repeated step hyperpolarization while monitoring the capacitance current transient due to charging the small membrane patch capacitor through the series resistance (mainly the electrode series resistor). If RubpyC17

dx.doi.org/10.1021/cn300213f | ACS Chem. Neurosci. 2013, 4, 585−593

permeabilizes the membrane of the attached patch, the conductance through the patch should increase, opening a path for current to charge the capacitor of the rest of the whole cell membrane; the capacitive charging transient should grow larger and the time constant of the decay should increase.

As shown in Figure 5F (top), we did not observe an increase in the capacitive charging transient, which indicates that RubpyC17 does not cause significant membrane damage. As a positive control, we performed the same experiment with amphotericin B, an antifungal antibiotic, which is used to create holes in cell membranes for perforated-patch experiments. Perforated-patch recordings allow current to flow through tiny holes in the membrane patch encircled by the pipet rim at the membrane, but prevent loss of critical cytosolic components (like ATP and proteins) from out of the cell and into the pipet. We use these recordings routinely to make recordings of action potentials. Within 5 min of gigaseal formation with amphotericin B in the pipet, we observed a sizable capacitive charging transient (Figure 5F, bottom), whereas with RubpyC17 we did not observe a noticeable change in the capacitance transients even 10 min after gigaseal formation (Figure 5F, top).

As a final test to rule out the possibility that membrane potential changes were due to pore formation, we replaced permeating ions (potassium and sodium) from our internal and external solution with nonpermeating ions (cesium and *N*-methyl-D-glucamine or NMDG). The light-triggered depolarization in RubpyC17-loaded INS cells still persisted when solutions containing nonpermeating ions were used (Figure 5G,H), thereby indicating that the membrane depolarization arises independent of transmembrane ion flux.

We have synthesized and characterized a photoactivatable nanoswitch RubpyC17 and demonstrated that it (1) integrates rapidly and stably into living cell membranes, (2) enables light-induced membrane potential changes, for which the direction of the change is dependent upon the nature (reductant versus oxidant) of a soluble redox partner present in solution, (3) facilitates light-induced changes in action potential firing rate in excitable cells, and (4) facilitates light-induced secretion from excitable secretory cells, such as chromaffin cells.

There are several notable differences between RubpyC17 and the other previously characterized small diffusible photoswitch compounds. Each has advantages and disadvanges, which may determine the choice for a particular application.

RubpyC17 integrates consistently, rapidly, and stably in the plasma membrane of a range of mammalian cells, including INS, HEK293, and primary cultured chromaffin cells. Based on its structure, RubpyC17 should be able to integrate into the membrane of most cell types. Screening for integration into cell membranes is rapid, because upon illumination RubpyC17 luminesces strongly in the red region of the visible spectrum, in contrast to azobenzene-based compounds that do not luminesce. Although ferrocene-porphyrin-C60 luminesces in solution, this radiative signature is quenched once delivered to the plasma membrane.[19] Having direct evidence that the complex is in the cell membrane speeds experimental protocols and enables ruling out absence of membrane-associated complex when a cell does not respond to illumination.

The mechanism of action of RubpyC17, unlike the azobenzene photoswitches, does not involve direct blocking or unblocking of specific ion channels. Rather, we suggest that the light-induced membrane potential change is the consequence of electron transfer to or from the ruthenium complex at the outer face of the cell membrane, which charges up the membrane capacitor and thereby indirectly activates or inhibits voltage-gated ion channels. This proposal is strongly supported by the observation that light induces depolarization in ruthenium complex-treated cells when ascorbate (reductant) is in the bath (Figure 2A,C,E), whereas light induces hyperpolarization when ferricyanide (oxidant) is in the bath (Figure 2A,G). Furthermore, ion channels are not needed for the membrane potential changes (Figure 5G,H), and membrane damage is not involved (Figure 5F). In contrast, the mechanism of action of soluble azobenzene photoswitches containing a quaternary ammonium moiety is light-induced unblocking and blocking of potassium channels.[18] Similarly, the mechanism of action of ferrocene-porphyrin-C60 is light-induced inhibition of potassium channels that only provides unidirectional control of membrane potential (light-induced depolarization).[19]

For maximum effect, the light-triggered depolarization in RubpyC17-treated cells requires on the order of 30 s of continuous illumination at 0.46−0.48 mE s^{-1} m^2 (Figure 2B−F). The time course observed is dependent on several factors. One, it is related to the probability of photon absorption per unit time by membrane-associated RubpyC17, which depends on the concentration of RubpyC17, the partitioning into the membrane, and the photon flux. Two, it is related to diffusional collision between the soluble redox partner and photoactivated RubpyC17, which depends on the density of the complex in the cell membrane and its membrane diffusion coefficient. Lastly, the time course is related to the probability of electron transfer in the case of a collision, and this also depends on the redox partner (i.e., ascorbate) not participating in competing redox reactions in the membrane or bath solution, which would reduce its effective concentration. Notably, electron transfer with ascorbate appears slower than with ferricyanide.[36−38] We suggest that the difference in kinetics is due to the higher efficiency of electron transfer from photoactivated RubpyC17 to ferricyanide ($k_{et} \sim 6.5 \times 10^9$ M^{-1} s^{-1} in aqueous solution), as compared to electron transfer from ascorbate ($k_{et} \sim 2 \times 10^7$ M^{-1} s^{-1}) to the photoactivated complex.[36−38]

The light-induced depolarization of RubpyC17-treated cells in the presence of reductants appears to be irreversible (Figure 2B−F) or reverses at a very slow rate (Figure 3A−C), as was reported also for ferrocene-porphyrin-C60. The irreversibility may be due to transfer of the electron from RubpyC17 to an endogenous membrane molecule that maintains the negative charge at the outer face of the cell membrane capacitor. The presence of endogeneous membrane components capable of participating in reduction−oxidation activity is likely, since RubpyC17-treated cells without the addition of excess reductant or oxidant still undergo depolarization in response to light (Figure 2A,D), though to a smaller extent than observed in the presence of a soluble redox partner.

Based on the continued viability of chromaffin cells after incubations of ∼30 min with RubpyC17, as evidenced by maintained light-induced action potential firing and secretion (Figure 3), it seems unlikely that RubpyC17 causes major nonspecific damage to the cell. The generation of nonspecific damage by light-activated RubpyC17 was ruled out by experiments showing that high concentrations of RubpyC17 failed to perforate the cell before or during light illumination, as measured in cell-attached mode (Figure 5D). Excessive and prolonged whole cell incubation with RubpyC17 (>10 μM for >5 min) may result in cell toxicity, since a stable gigaseal cannot

be maintained in those cells. At this time, we do not yet know the mechanism behind the adverse effects on cell health upon RubpyC17 overexposure. Since we did not achieve perforation when a small patch of membrane was exposed to a high dose of RupbyC17, we suggest that when an entire cell is overexposed to RubpyC17, there may be sufficient random interactions between excess RubpyC17 complex and endogenous surface molecules (i.e., proteins, carbohydrates, sugars), triggering signals that lead to cell health deterioration. However, when used in its appropriate dose range, RubpyC17 is tolerated by cells and consistently confers light sensitivity.

In summary, metal-diimine complexes are photoactivatable nanoswitches that serve as a convenient tool for remote optical control of cellular electrical activity. Unlike the prevailing tools for remote optical control, the metal-diimine complexes do not require expression of high levels of a foreign protein or excitation by cytotoxic wavelengths. The potential for analog control by varying light illumination intensity and duration using this complex is worth exploring. We do have preliminary data showing that increasing the ferricyanide concentration from 0.1 to 0.2 mM further suppressed action potential firing. The current photoactivatable nanoswitches do not offer rapid on−off switching of cellular electrical activity, but future generations in which both electron donor and acceptor moieties are joined in a single molecule may overcome some of these limitations.

METHODS

Synthesis of $[Ru(bpy)_2(bpy\text{-}C17)](PF_6)_2$. RubpyC17 refers to the compound $[Ru(bpy)_2(bpy\text{-}C17)](PF_6)_2$. In our work, a 17-carbon tail has been conjugated to one of the three bipyridines to allow for stable insertion into the plasma membrane (Figure 1A). The bpy-C17 ligand was synthesized following reported procedures.[29,39] Briefly, 0.7 mL of lithium diisopropylamide (LDA) (2 M) was added dropwise to a cold tetrahydrofuran (THF) solution of 4,4′-dimethyl-2,2.-bipyridine (0.25 g, 1.3 mmol) under an argon atmosphere. After 30 min, into this brown solution was cannulated a solution of dry THF containing 1-bromohexadecane (0.46 g, 1.5 mmol). After the reaction mixture had been stirred for several hours at room temperature, the solvent was removed under vacuum. The residue was then dissolved in CH_2Cl_2 and washed with 150 mL of brine. The product was isolated as an off-white powder. Yield: 345 mg, 65%. The desired metal complex was prepared by refluxing for 3 h a methanol solution containing bpy-C17 ligand (0.10 g, 0.25 mmol) and $Ru(bpy)_2Cl_2$ (0.09 g, 0.21 mmol) and was isolated as the PF_6 salt. The experimentally determined mass for the product is m/z = 411.195 $[M^{2+}]$ (calculated: 411.196). ^{1}H NMR (DMSO-d_6, 400 MHz): 8.82 (4H, d), 8.76 (1H, d), 8.70 (1H, d), 8.15 (4H, t), 7.72 (4H, q), 7.53 (6H, m), 7.37 (2H, t), 2.07 (5H, s), 1.25 (30H, m), 0.84 (3H, t). All absorption and emission measurements were conducted in degassed 5% DMSO/aqueous solution. UV−vis absorption spectra were collected using a Cary-50 spectrophotometer. Luminescence spectra were obtained using a Jobin Yvon Spex Fluorolog-3-11 instrument. Sample excitation was achieved via a xenon arc lamp with a monochromator providing wavelength selection. The excitation wavelength was scanned between 300 and 560 nm and recorded at 580 nm. Slits of 1 nm bandpass were used for excitation and emission.

Culture of HEK and INS Cells. HEK-293T cells were cultured on glass-bottomed culture dishes in DMEM medium supplemented with 10% fetal bovine serum, 1% penicillin/streptomycin and kept in a humid incubator at 5% CO_2. The INS-1 823/13 cells (pancreatic insulin-producing cells, a gift from Chris Newgard) were cultured on glass-bottomed culture dishes in RPMI-1640 medium supplemented with 10% fetal calf serum, 10 mM HEPES, 2 mM L-glutamine, 1 mM sodium-pyruvate, and 0.05 mM 2-mercaptoethanol and kept in a humid incubator at 5% CO_2. Fetal bovine serum, fetal calf serum, penicillin/streptomycin, DMEM, and RPMI-1640 were purchased from Invitrogen. Other chemicals were purchased from Sigma.

Preparation of Mouse Chromaffin Cells. Mouse adrenal chromaffin cells were dissected from 1−3 month old C57BL/6J mice and were prepared as follows: (1) adrenal glands were removed and placed in cold mouse buffer on ice, (2) fat layers and cortex were removed, and (2) medullae were digested by papain followed by collagenase, at 37 °C. Chromaffin cells were plated on matrigel-coated coverslips and placed in a humid incubator, with 5% CO_2. Chromaffin cells were patch clamped the next 2 days following dissection. Mouse buffer consisted of Locke's solution (154 mM NaCl, 2.6 mM KCl, 2.2 mM $K_2HPO_4.3H_2O$, 0.85 mM KH_2PO_4) supplemented with 10 mM dextrose, 5 mM HEPES free acid, 3.7 mM mannitol, and 0.1% phenol red, bubble with 95%/5% O_2−CO_2 for 10 min, pH to 7.2, adjust osmolarity (with mannitol) to 320 mOsm, and then add in sterile hood 0.4% gentamycin and 0.4% pen/strep antibiotics. Papain was dissolved in mouse buffer at 25−30 U/mL. Collagenase solution consisted of 3 mg/mL collagenase (Worthington) in mouse buffer supplemented with 100 μM $CaCl_2$ in mouse buffer. Complete medium consisted of DMEM supplemented with 10% ITS-X (Invitrogen), 10% AraC, 1% gentamycin, 1% pen/strep, 1% FdU, and 10% L-glutamine. Matrigel (BD Biosciences) was diluted 1:8 in DMEM, applied to coverslips for ∼1 h, and then washed 3× with DMEM.

Imaging RubpyC17 in Live Cells. Cells were imaged at 1−3 days after plating. The glass-bottomed chambers with adherent cells were washed twice with PBS and then filled with standard extracellular solution consisting of 140 mM NaCl, 2.8 mM KCl, 10 mM HEPES, 1 mM $MgCl_2$, 2 mM $CaCl_2$, and 10 mM glucose, with pH adjusted to 7.2−7.4 and osmolarity adjusted to 290−310 mOsm. The chamber was then mounted on an Olympus IX70 inverted microscope stage for imaging, using a Cascade 512B EMCCD camera, operated by Metamorph software. Initial imaging was done with cells in extracellular solution without RubpyC17, first under brightfield to evaluate cell health and morphology, and then under widefield argon ion laser illumination at 488 nm (Coherent, Innova 90-5, Santa Clara, CA) to evaluate autofluorescence. Next, the extracellular solution was removed and replaced with extracellular solution containing RubpyC17 (10 μM in ≤0.01% DMSO, final concentrations). Cell images were then acquired with illumination at 488 nm (collected with a long-pass red emission filter). For electrophysiological experiments, RubpyC17 was added to the extracellular solution (2−10 μM in ≤0.01% DMSO, final concentrations as indicated) and cells were incubated for 1.5−45 min, as indicated, and then washed with extracellular solution without RubpyC17. Some chromaffin cells were also exposed continuously to 490−900 nM RubpyC17-containing extracellular solution.

Whole Cell Patch Clamp Electrophysiology. Membrane potential was monitored using whole cell patch clamp in current-clamp mode. Cultured cells (INS and HEK293) were plated on a glass-bottomed culture dishes 1−3 days prior to recording. Cells were incubated in standard extracellular solution with or without 10 μM RubpyC17 for approximately 1.5−2 min, then washed and incubated with standard extracellular solution without additional supplementation, or with 2−5 mM ascorbate, 100 μM sodium ferrocyanide, or 100−200 μM potassium ferricyanide, as indicated. The chamber was transferred to the microscope stage. Extracellular solution consisted of 140 mM NaCl, 2.8 mM KCl, 10 mM HEPES, 1 mM $MgCl_2$, 2 mM $CaCl_2$, and 10 mM glucose, with pH adjusted to 7.3 and osmolarity adjusted to 300−310 mOsm. Conventional whole-cell patch clamp recordings were performed with an EPC-9 amplifier and Pulse software (HEKA Electronics). Pipette electrodes of 1.8−3.5 MΩ were fire polished before use. Intracellular solution consisted of 145 mM KCl, 10 mM NaCl, 1 mM $MgCl_2$, 1 mM EGTA, 2 mM ATP, 0.3 mM GTP, and 10 mM HEPES, with pH adjusted to 7.3 and osmolarity adjusted to 290−300 mOsm. To monitor changes in membrane voltage/potential, cells were patch clamped in current-clamp mode. Access resistances were in the range of 3−8 MΩ. Using Pulse, membrane potentials were recorded before, during, and after illumination by the argon ion laser at 488 nm with an irradiance value of 0.458 mE s^{-1} m^{-2} or by a xenon lamp source through a 470/

dx.doi.org/10.1021/cn300213f | ACS Chem. Neurosci. 2013, 4, 585−593

40 nm bandpass excitation filter with an irradiance value of 0.480 mE s^{-1} m^{-2}. The duration of illumination varied and the timing is indicated by bars on the figures.

Perforated Patch Clamp Electrophysiology. Action potentials in chromaffin cells were monitored using perforated patch clamp electrophysiology in current-clamp mode, using an EPC10 amplifer and Patchmaster data acquisition software (HEKA electronics). A coverslip containing mouse chromaffin cells was transferred to a recording chamber and perfused with extracellular solution. Extracellular solution consisted of 140 mM NaCl, 2.8 mM KCl, 10 mM HEPES, 1 mM $MgCl_2$, 2 mM $CaCl_2$, and 10 mM glucose, with pH adjusted to 7.3 and osmolarity adjusted to 290−300 mOsm. Intracellular solution consisted of 145 mM KCl, 10 mM NaCl, 1 mM $MgCl_2$, and 10 mM HEPES, with pH adjusted to 7.3 and osmolarity adjusted to 290−300 mOsm. Perforation solution was prepared by adding 4.5 μL of 125 mg/mL stock of amphoterecin B (Sigma) in DMSO to 1.8 mL of intracellular solution and homogenizing for 5−10 s. Perforation was achieved within 3−10 min following gigaseal formation. Series resistances were in the range of 8−22 MΩ. Light stimulation in the blue region of the spectrum originated from a xenon lamp source with an irradiance value of 0.480 mE s^{-1} m^{-2} through a 470/40 nm bandpass excitation filter. The duration of illumination varied, as indicated by bars on the figures.

Amperometry. Carbon fiber electrodes were prepared as previously described[33,34] and coupled to an EPC10 amplifier. A +800 mV constant voltage was applied to the electrode relative to the Ag/AgCl bath electrode. The amperometry recordings were sampled at 4 kHz using Pulsemaster (HEKA). Extracellular composition consisted of 120 mM NaCl, 20 mM KCl, 10 mM HEPES, 1 mM $MgCl_2$, 2 mM $CaCl_2$, and 10 mM glucose, with pH adjusted to 7.2−7.4 and osmolarity adjusted to 290−300 mOsm. Light stimulation in the blue spectrum originated from a xenon lamp source through a 470/40 nm bandpass excitation filter. The duration of illumination varied and is indicated by bars on figures.

Data Analysis. Data, which are represented as means with the standard error of the mean (SEM), were statistically compared using unpaired, two-tailed Student's *t* test.

AUTHOR INFORMATION

Corresponding Author

*Telephone: (323) 442-2901. Fax: (323) 442-4466. E-mail: rchow@usc.edu.

Author Contributions

J.G.R. and Y.R.C. contributed equally to the manuscript. M.H. and R.H.C. designed the study. A.C.D. and L.E.C. synthesized and characterized the ruthenium-diimine compound. J.G.R. and Y.R.C. conducted the electrophysiological and imaging experiments. J.G.R., Y.R.C., and R.H.C. wrote the manuscript. All authors participated in the discussion of data and revision of manusccript.

Author Contributions

○The first two authors contributed equally to this work.

Funding

The present work was supported by the following funding agencies NSF ERC EEC-0310723 (M.H., R.H.C.), Beckman Initiative for Macular Research Grant 1113 (V.P., R.H.C.), Doheny Eye Institute through the Arnold and Mabel Beckman Foundation (M.H., R.H.G.), NIH RO1 GM85791 (R.H.C.), NIH DK019038 (H.B.G.), and NIH F32GM088967 (J.G.R.).

Notes

The authors declare no competing financial interest.

REFERENCES

(1) Caporale, N., Kolstad, K. D., Lee, T., Tochitsky, I., Dalkara, D., Trauner, D., Kramer, R., Dan, Y., Isacoff, E. Y., and Flannery, J. G. (2011) LiGluR Restores Visual Responses in Rodent Models of Inherited Blindness. *Mol. Ther. 19*, 1212−1219.

(2) Banghart, M., Borges, K., Isacoff, E., Trauner, D., and Kramer, R. H. (2004) Light-activated ion channels for remote control of neuronal firing. *Nat. Neurosci. 7*, 1381−1386.

(3) Chambers, J. J., Banghart, M. R., Trauner, D., and Kramer, R. H. (2006) Light-Induced Depolarization of Neurons Using a Modified Shaker K+ Channel and a Molecular Photoswitch. *J. Neurophysiol. 96*, 2792−2796.

(4) Tochitsky, I., Banghart, M. R., Mourot, A., Yao, J. Z., Gaub, B., Kramer, R. H., and Trauner, D. (2012) Optochemical control of genetically engineered neuronal nicotinic acetylcholine receptors. *Nat. Chem. 4*, 105−111.

(5) Fortin, D. L., Banghart, M. R., Dunn, T. W., Borges, K., Wagenaar, D. A., Gaudry, Q., Karakossian, M. H., Otis, T. S., Kristan, W. B., Trauner, D., and Kramer, R. H. (2008) Photochemical control of endogenous ion channels and cellular excitability. *Nat. Methods. 5*, 331−338.

(6) Bi, A., Cui, J., Ma, Y.-P., Olshevskaya, E., Pu, M., Dizhoor, A. M., and Pan, Z.-H. (2006) Ectopic Expression of a Microbial-Type Rhodopsin Restores Visual Responses in Mice with Photoreceptor Degeneration. *Neuron 50*, 23−33.

(7) Boyden, E. S., Zhang, F., Bamberg, E., Nagel, G., and Deisseroth, K. (2005) Millisecond-timescale, genetically targeted optical control of neural activity. *Nat. Neurosci. 8*, 1263−1268.

(8) Busskamp, V., Duebel, J., Balya, D., Fradot, M., Viney, T. J., Siegert, S., Groner, A. C., Cabuy, E., Forster, V., Seeliger, M., Biel, M., Humphries, P., Paques, M., Mohand-Said, S., Trono, D., Deisseroth, K., Sahel, J. A., Picaud, S., and Roska, B. (2010) Genetic Reactivation of Cone Photoreceptors Restores Visual Responses in Retinitis Pigmentosa. *Science 329*, 413−417.

(9) Gradinaru, V., Thompson, K. R., and Deisseroth, K. (2008) eNpHR: a Natronomonas halorhodopsin enhanced for optogenetic applications. *Brain Cell Biol. 36*, 129−139.

(10) Kramer, R. H., Fortin, D. L., and Trauner, D. (2009) New photochemical tools for controlling neuronal activity. *Curr. Opin. Neurobiol. 19*, 544−552.

(11) Lagali, P. S., Balya, D., Awatramani, G. B., Münch, T. A., Kim, D. S., Busskamp, V., Cepko, C. L., and Roska, B. (2008) Light-activated channels targeted to ON bipolar cells restore visual function in retinal degeneration. *Nat. Neurosci. 11*, 667−675.

(12) Lin, B., Koizumi, A., Tanaka, N., Panda, S., and Masland, R. H. (2008) Restoration of visual function in retinal degeneration mice by ectopic expression of melanopsin. *Proc. Natl. Acad. Sci. U.S.A. 105*, 16009−16014.

(13) Prigge, M., Schneider, F., Tsunoda, S. P., Shilyansky, C., Wietek, J., Deisseroth, K., and Hegemann, P. (2012) Color-tuned Channelrhodopsins for Multiwavelength Optogenetics. *J. Biol. Chem. 287*, 31804−31812.

(14) Zemelman, B. V., Lee, G. A., Ng, M., and Miesenbock, G. (2002) Selective Photostimulation of Genetically ChARGed Neurons. *Neuron 33*, 15−22.

(15) Zhang, F., Wang, L.-P., Boyden, E. S., and Deisseroth, K. (2006) Channelrhodopsin-2 and optical control of excitable cells. *Nat. Methods 3*, 785−792.

(16) Callaway, E. M., and Yuste, R. (2002) Stimulating neurons with light. *Curr. Opin. Neurobiol. 12*, 587−592.

(17) Kandler, K., Katz, L. C., and Kauer, J. A. (1998) Focal photolysis of caged glutamate produces long-term depression of hippocampal glutamate receptors. *Nat. Neurosci. 1*, 119−123.

(18) Polosukhina, A., Litt, J., Tochitsky, I., Nemargut, J., Sychev, Y., De Kouchkovsky, I., Huang, T., Borges, K., Trauner, D., Van Gelder, R. N., and Kramer, R. H. (2012) Photochemical Restoration of Visual Responses in Blind Mice. *Neuron 75*, 271−282.

(19) Numata, T., Murakami, T., Kawashima, F., Morone, N., Heuser, J. E., Takano, Y., Ohkubo, K., Fukuzumi, S., Mori, Y., and Imahori, H. (2012) Utilization of Photoinduced Charge-Separated State of Donor−Acceptor-Linked Molecules for Regulation of Cell Membrane Potential and Ion Transport. *J. Am. Chem. Soc. 134*, 6092−6095.

(20) Chang, I.-J., Gray, H. B., and Winkler, J. R. (1991) High-Driving-Force Electron Transfer in Metalloproteins: Intramolecular Oxidation of Ferrocytochrome *c* by $Ru(2,2'\text{-bpy})_2(im)(His\text{-}33)^{3+}$. *J. Am. Chem. Soc. 113*, 7056−7057.
(21) Dunn, A. R., Belliston-Bittner, W., Winkler, J. R., Getzoff, E. D., Stuehr, D. J., and Gray, H. B. (2005) Luminescent Ruthenium(II)- and Rhenium(I)-Diimine Wires Bind Nitric Oxide Synthase. *J. Am. Chem. Soc. 127*, 5169−5173.
(22) Elias, H., Chou, M. H., and Winkler, J. R. (1988) Electron-Transfer Kinetics of Zn-Substituted Cytochrome c and Its Ru(NH3-(Histidine-33) Derivative. *J. Am. Chem. Soc. 110*, 429−434.
(23) Ener, M. E., Lee, Y.-T., Winkler, J. R., Gray, H. B., and Cheruzel, L. (2010) Photooxidation of cytochrome P450-BM3. *Proc. Natl. Acad. Sci. U.S.A. 107*, 18783−18786.
(24) Immoos, C. E., Bilio, A. J. D., Cohen, M. S., Veer, W. V. d., Gray, H. B., and Farmer, P. J. (2004) Electron-Transfer Chemistry of Ru-Linker-(Heme)-Modified Myoglobin: Rapid Intraprotein Reduction of a Photogenerated Porphyrin Cation Radical. *Inorg. Chem. 43*, 3593−3596.
(25) Nocera, D. G., Winkler, J. R., Yocom, K. M., Bordignon, E., and Gray, H. B. (1984) Kinetics of Intramolecular Electron Transfer from Ru^{II} to Fe^{III} in Ruthenium-Modified Cytochrome *c*. *J. Am. Chem. Soc. 106*, 5145−5150.
(26) Whited, C. A., Belliston-Bittner, W., Dunn, A. R., Winkler, J. R., and Gray, H. B. (2008) Probing the heme-thiolate oxygenase domain of inducible nitric oxide synthase with Ru(II) and Re(I) electron tunneling wires. *J. Porphyrins Phthalocyanines 12*, 971−978.
(27) Whited, C. A., Belliston-Bittner, W., Dunn, A. R., Winkler, J. R., and Gray, H. B. (2009) Nanosecond photoreduction of inducible nitric oxide synthase by a Ru-diimine electron tunneling wire bound distant from the active site. *J. Inorg. Biochem. 103*, 906−911.
(28) Winkler, J. R., Nocera, D. G., Yocom, K. M., Bordignon, E., and Gray, H. B. (1982) Electron-Transfer Kinetics of Pentaammineruthenium(II1) (histidine-33)-Ferricytochrome c. Measurement of the Rate of Intramolecular Electron Transfer between Redox Centers Separated by 15 angstroms, in a Protein. *J. Am. Chem. Soc. 104*, 5798−5800.
(29) Dunn, A., Dmochowski, I., Winkler, J., and Gray, H. (2003) Nanosecond Photoreduction of Cytochrome P450cam by Channel-specific Ru-diimine Electron Tunneling Wires. *J. Am. Chem. Soc. 125*, 12450−12456.
(30) Durham, B., and Millett, F. (2012) Design of photoactive ruthenium complexes to study electron transfer and proton pumping in cytochrome oxidase. *Biochim. Biophys. Acta, Bioenerg. 1817*, 567−574.
(31) Marin, V., Holder, E., Hoogenboom, R., and Schubert, U. S. (2007) Functional ruthenium(ii)- and iridium(iii)-containing polymers for potential electro-optical applications. *Chem. Soc. Rev. 36*, 618.
(32) Hoffman, M. Z., Bolletta, F., Moggi, L., and Hug, G. L. (1989) Rate Constants for the Quenching of Excited States of Metal Complexes in Fluid Solution. *J. Phys. Chem. Ref. Data 18*, 219−543.
(33) Schulte, A., and Chow, R. H. (1998) Cylindrically Etched Carbon-Fiber Microelectrodes for Low-Noise Amperometric Recording of Cellular Secretion. *Anal. Chem. 70*, 985−990.
(34) Schulte, A., and Chow, R. H. (1996) A Simple Method for Insulating Carbon-Fiber Microelectrodes Using Anodic Electrophoretic Deposition of Paint. *Anal. Chem. 68*, 3054−3058.
(35) Rae, J., Cooper, K., Gates, P., and Watsky, M. (1991) Low access resistance perforated patch recordings using amphotericin B. *J. Neurosci. Methods 37*, 15−26.
(36) Creutz, C., and Sutin, N. (1976) Electron Transfer Reactions of Excited States: Reductive Quenching of the Tris(2,2′-bipyridine)-ruthenium(II) Luminescence. *Inorg. Chem. 15*, 496−499.
(37) Creutz, C., Sutin, N., and Brunschwig, B. S. (1979) Excited-state photochemistry in the tris(2,2′-bipyridine)ruthenium(II)-sulfite system. *J. Am. Chem. Soc. 101*, 1297−1298.
(38) Lin, C. T., and Sutin, N. (1976) Quenching of the Luminescence of the Tris(2,2′-bipyridine) Complexes of Ruthenium-(II) and Osmium(II): Kinetic Considerations and Photogalvanic Effects. *Phys. Chem. 80*, 97−105.
(39) Wilker, J. J., Dmochowski, I. J., Dawson, J. H., Winkler, J. R., and Gray, H. B. (1999) Substrates for Rapid Delivery of Electrons and Holes to Buried Active Sites in Proteins. *Angew. Chem., Int. Ed. 38*, 90−92.